

Investigations on doping of amorphous and nanocrystalline silicon films deposited by catalytic chemical vapour deposition

M. Fonrodona¹, D. Soler, J. Bertomeu and J. Andreu

Universitat de Barcelona. Departament de Física Aplicada i Òptica.

Av. Diagonal 647, 08028-Barcelona, Catalonia, Spain.

Abstract

Hydrogenated amorphous and nanocrystalline silicon, deposited by catalytic chemical vapour deposition, have been doped during deposition by the addition of diborane and phosphine in the feed gas, with concentrations in the range of 1%. The crystalline fraction, dopant concentration and electrical properties of the films are studied. The nanocrystalline films exhibited a high doping efficiency, both for n and p doping, and electrical characteristics similar to those of plasma-deposited films. The doping efficiency of n-type amorphous silicon is similar to that obtained for plasma-deposited electronic grade amorphous silicon, whereas p-type layers show a doping efficiency one order of magnitude lower. A higher deposition temperature of 450°C has been required to achieve p-type films with electrical characteristics similar to those of plasma-deposited films.

Keywords: Catalytic Chemical Vapour Deposition; Nanocrystalline silicon; Amorphous silicon; Doping efficiency

¹Corresponding author: Phone: +34 93 402 11 34, Fax: +34 93 402 11 38, E-mail: marta@fao.ub.es

1. Introduction

Efficient doping of amorphous and nanocrystalline silicon is a key issue to fabricate thin film silicon based devices, such as solar cells or thin film transistors. Intrinsic amorphous and nanocrystalline silicon deposited by Catalytic Chemical Vapour Deposition (Cat-CVD) is being intensively studied in order to apply these materials to devices. Most of the devices incorporating intrinsic active layers produced by Cat-CVD use heavily doped contact layers produced by plasma enhanced CVD (PECVD) [1], and consequently benefit from the wide experience of such a mature technique. Cat-CVD features several advantages with respect to PECVD, such as the higher deposition rates achieved, the lack of ion bombardment and the ability to produce atomic hydrogen [2]. Whereas the first advantage is not relevant to device fabrication, since doped layers are usually very thin, the others could result in improvements in the performance of devices fabricated by Cat-CVD. In spite of these potential advantages, only a few studies on doped silicon thin films deposited by this technique have been published [3-8], and more effort in the study of doped material produced by Cat-CVD should be done.

In this paper, the doping efficiency of amorphous and nanocrystalline silicon samples deposited by Cat-CVD is presented. New results on the doping efficiency of p-type amorphous silicon obtained at high substrate temperature (450°C) and high filament temperature (1900°C) are presented. Under these conditions, the doping efficiency is the same than that of PECVD samples. This efficiency cannot be reached at lower substrate temperatures (200-300°C). Some possible reasons for this behaviour are also discussed.

2. Sample preparation and experimental procedures

The samples were deposited in a Cat-CVD setup described elsewhere [9]. Five samples were deposited at substrate temperatures between 125 and 225°C onto Corning glass and c-Si wafers, using the conditions summarised in Table 1. A basket-shaped tungsten filament, with three coils (0.5 mm diameter and 10 cm length), was used. Another p-type amorphous sample (AP2) was deposited at higher substrate temperature, higher silane flow, and with a straight filament (0.5 mm diameter and 4 cm length). These parameters lead to device quality amorphous silicon films [10]. All the films were doped by adding B or P atoms from diborane or phosphine, with ratios to Si atoms in the order of 1% in the gas phase. The labels of the films indicate their structural nature (A or C for amorphous or nanocrystalline, respectively), and the type of doping used (P or N for p-type or n-type, respectively).

Samples CN and CP1 were prepared under selected deposition conditions that produce good nanocrystalline intrinsic material. Sample CP2 was deposited with a lower gas phase boron concentration, with deposition conditions optimised to obtain higher crystallinity [7]. This optimisation has led to a lower deposition temperature. Finally, a-Si:H samples AN and AP1 have been deposited at low temperatures and AP2 at a moderately high temperature.

The structure of the films was analysed by Raman measurements, and their crystalline fraction (X_C) was determined by deconvoluting the amorphous and crystalline contributions to the TO-phonon band.

The dopant incorporation has been analysed by secondary ion mass spectrometry

(SIMS). The samples were bombarded with O^{2+} ions accelerated at 12 kV, and depth profiles reaching the substrate were measured. In order to obtain the boron and phosphorus densities in the films from SIMS signals, two implanted c-Si wafers with well known B and P densities were analysed under the same conditions. B (mass 11) to Si (mass 30), and P (mass 31) to Si (mass 30) signal ratios were used to deduce the solid phase concentration of dopants in the films.

Standard coplanar measurements of the resistance, in the temperature range between 30 and 150°C, were performed to determine the activation energy (E_A) of the dark conductivity.

3. Results

The Raman spectra of all samples are presented in Fig. 1. The amorphous structure of samples AN, AP1 and AP2, was evidenced by the presence of a broad peak centred at 480 cm^{-1} , without a trace of a peak at 520 cm^{-1} . Samples CN, CP1 and CP2 demonstrated crystallinity, as seen by the presence of the contribution at 520 cm^{-1} . The crystalline fractions of the films are shown in Table 2. Whereas samples CN and CP2 exhibit very similar values of X_C , sample CP1 exhibits a higher amorphous phase contribution. Since samples CN and CP1 were deposited at the same conditions except for the type of dopant (phosphorus for CN and boron for CP1), the difference between their structures has been attributed to amorphisation induced by the presence of high concentrations of boron. Further experimental work has demonstrated that the decrease in the crystallinity of the p-type samples with the increase of boron concentration in the gas phase can be avoided with optimized deposition

conditions [7].

SIMS analysis of these samples showed a slightly lower incorporation efficiency of dopant atoms in the solid phase for the case of n-type films. B concentrations between $6 \times 10^{20} \text{ cm}^{-3}$ and $1.2 \times 10^{21} \text{ cm}^{-3}$ were obtained for the p-type films, whereas P concentrations in the range of $1 \times 10^{20} \text{ cm}^{-3}$ were obtained for the n-type films.

As far as electrical properties are concerned, the dark conductivities of the films at 30°C , and the activation energies deduced from Arrhenius plots are summarised in Table 2. In Fig. 2, Arrhenius plots corresponding to p-type samples are shown. Data were taken while heating from room temperature, and also while cooling down to room temperature. Activation energy values were deduced for the cooling part of the plots in all cases.

4. Discussion

A good starting point to obtain doped nanocrystalline silicon films should be the addition of the suitable amount of doping gas during the deposition process, while maintaining all the technological parameters that lead to an intrinsic material with good structural and optoelectrical properties. This approach is appropriate in the case of n-type nc-Si:H films, in which highly conductive samples in the range of 10 S cm^{-1} have been obtained at low temperatures.

In the case of p-type nc-Si:H films this approach is no longer valid, especially when high B doping levels are used. It has been reported that the incorporation of B to the films

leads to smaller crystalline fraction and grain size [5,7]. Certain deposition conditions can overcome this effect. In particular, the lower substrate temperature (125°) of sample CP2 favours a higher crystallinity. This can be attributed to surface passivation of the growing layer by atomic hydrogen, which is higher at lower temperatures. Regardless of the technological conditions used in the deposition process, a correlation between the dark conductivity and the crystalline fraction is observed for samples deposited at low temperatures (<300°C) for boron concentrations in the gas phase close to 1% (Fig. 3). The conductivity of sample CP2 at 30°C is 1.7 S cm^{-1} , which is nearly the same as reported elsewhere [5, 11] for nanocrystalline samples with high crystalline fractions, deposited by Cat-CVD in the same range of temperatures and concentrations.

It is interesting to point out that the high dopant concentration in the films CN and CP2 leads to degenerated samples. The activated behaviour of their conductivity is probably due to an activation of the mobility. The conductivity of a crystalline silicon wafer with a dopant concentration similar to that of the n-doped sample CN (10^{20} cm^{-3}) would be 10^3 S cm^{-1} [12]. The difference (a factor of 100) between the conductivity of this nanocrystalline film and that of a pure crystalline material can be attributed to the lower mobility of the former. By using the SIMS measured P concentration in this film as the density of carriers, and a field-effect mobility value of $0.7 \text{ cm}^2 \text{ V}^{-1} \text{ s}^{-1}$, that we previously measured from thin film transistors [13], a dark conductivity of 11 S cm^{-1} could be expected. This value is nearly the same as the 9.7 S cm^{-1} measured value. This points to a doping efficiency close to 100%. For the p-type sample CP2, from the B concentration of 10^{21} cm^{-3} measured by SIMS and by assuming the same mobility value, the expected conductivity would be 110 S cm^{-1} , which is much higher than the 1.7 S cm^{-1} value measured for this sample. This larger difference between p- and n-doping

appears to imply a segregation of B atoms towards the grain boundaries, thus leading to a doping efficiency around 1%. Higher doping efficiencies have been reported for p-type films deposited by Cat-CVD at higher substrate temperatures [6]. This points to a lower solubility limit of the B atoms in the crystallites at these low temperatures.

In spite of this low doping efficiency observed for p-type films, the dark conductivity of the optimised sample CP2 is very similar to the best ones obtained for nc-Si:H films deposited by other techniques at similar temperatures. Moreover, it has been proved that Cat-CVD can produce thin (≈ 100 nm) nc-Si:H films with conductivities in the order of 1 S cm^{-1} at low temperature deposition conditions [7,11], which are suitable to be used as degenerated semiconductors for contact purposes while maintaining a low deposition temperature. This high conductivity for such thin films has been attributed to the absence of a significant amorphous incubation layer.

As far as a-Si:H films are concerned, the conductivity of the n-type amorphous sample (AN) is $1.6 \times 10^{-2} \text{ S cm}^{-1}$. This value is similar to that of plasma deposited samples obtained with the same gas phase concentration of phosphine [14]. For sample AP1, the conductivity is $3.3 \times 10^{-6} \text{ S cm}^{-1}$, which is an order of magnitude lower than in PECVD samples with the same dopant concentration. We have deposited a p-type amorphous sample with one order of magnitude less dopant incorporation in the gas phase and its conductivity is still one order of magnitude lower than that of corresponding PECVD samples. A similar result has been reported elsewhere [5]. This lower conductivity cannot be attributed to a lower incorporation of dopant in Cat-CVD than in PECVD. SIMS measurements of dopant concentrations in p-type amorphous samples, with boron gas phase concentrations around 1 and 2 %, gave dopant

solid phase densities between $6 \times 10^{20} \text{ cm}^{-3}$ and $1.2 \times 10^{21} \text{ cm}^{-3}$. Therefore, the lower conductivity of Cat-CVD p-type samples should be attributed to a lower doping efficiency than for PECVD deposited samples. This fact could be due to a poorer structure of these films with respect to that of PECVD ones, as suggested by the high Urbach energy value (65 meV) obtained for intrinsic a-Si:H films deposited by Cat-CVD under the same conditions. By using other deposition conditions (higher substrate temperature, lower filament surface and higher silane flow), which lead to a Urbach energy value of 54 meV for intrinsic films, a higher conductivity of $9.1 \times 10^{-6} \text{ S cm}^{-1}$ and a lower activation energy of 0.47 eV were obtained for sample AP2. These values are similar to those obtained by PECVD, and show that the lower boron doping efficiency observed in low temperature Cat-CVD samples is likely related to structural defects in the material, which can be minimised by a proper tuning of technological parameters.

5. Conclusions

Nanocrystalline silicon obtained by Cat-CVD can efficiently be doped, both p and n-type, with the incorporation of B_2H_6 and PH_3 in the gas phase. Dark conductivities of 9.7 S cm^{-1} and 1.7 S cm^{-1} have been obtained, respectively, for n and p-type nc-Si:H samples deposited at temperatures below 250°C . Heavy p-type doping favours the growth of samples with a higher amorphous phase. This effect can be avoided by selecting appropriate deposition conditions. From the analysis of the dopant incorporation in the film, doping efficiencies close to 100% and to 1% were estimated, respectively, for n and p-type nc-Si:H films deposited at low temperatures. The lower doping efficiency in p-type samples has been attributed to the segregation of B atoms at the grain boundaries.

Amorphous silicon films can be grown both p and n-type at low temperature by Cat-CVD. Whereas n-type doping with Cat-CVD presents a doping efficiency similar to that observed in PECVD, p-type doping is one order of magnitude less efficient, and moderately high substrate temperatures (450°C) are required with Cat-CVD to obtain the same doping efficiency as opposed to PECVD.

Aknowledgements

This work has been financed by the Spanish Government (TIC98-0381-C02-01). The authors thank the Scientific-Technical Services of the UB for Raman measurements and the SIMS service of the UB.

References

- [1] R.E.I. Schropp, J.K. Rath, IEEE Trans. Electron Devices 46 (1999) 2069.
- [2] H. Matsumura, Jpn. J. Appl. Phys. 37 (1998) 3175.
- [3] J. Puigdollers, J. Cifre, M.C. Polo, J.M. Asensi, J. Bertomeu, J. Andreu, A. Lloret, Appl. Surf. Sci. 86 (1995) 600.
- [4] H.N. Wanka, R. Zedlitz, M. Heintze, M.B. Schubert, in: W. Freiesleben, W. Palz, H.A. Ossenbrink, P. Helm (Eds.), Proceedings of the Thirteenth European Photovoltaic Solar Energy Conference, Vol. II, H.S. Stephens & Associates, Bedford, 1995, p. 1753.
- [5] P. Brogueira, V. Chu, A.C. Ferro, J.P. Conde, J. Vac. Sci. Technol. A 15 (1997) 2968.
- [6] R. Brüggeman, A. Hierzenberger, P. Reinig, M. Rojahn, M.B. Schubert, S. Schweizer, H.N. Wanka, I. Zrinscak, J. Non-Cryst. Solids 227/230 (1988) 982.
- [7] C. Voz, D. Peiró, J. Bertomeu, D. Soler, M. Fonrodona, J. Andreu: Mater. Sci. Eng. B 69/70 (2000) 278.
- [8] S.R. Jadkar, J.V. Sali, M.G. Takwale, D.V. Musale, S.T. Kshirsagar, Sol. Energy Mater. Sol. Cells 64 (2000) 333.

- [9] C. Voz, D. Peiró, M. Fonrodona, D. Soler, J. Bertomeu, J. Andreu, Sol. Energy Mater. Sol. Cells 63 (2000) 237.
- [10] A.H. Mahan, J. Carapella, B.P. Nelson, R.S. Crandall, I. Balberg, J. Appl. Phys. 69 (1991) 6728.
- [11] J. Guillet, C. Niikura, J.E. Bourée, J.P. Kleider, C. Longeaud, R. Brüggemann, Mat. Sci. Eng. B 69/70 (2000) 284.
- [12] S.M. Sze, Physics of semiconductor Devices, 2nd Edition, John Wiley & Sons, New York, 1981, p. 32.
- [13] J. Puigdollers, D. Dosev, A. Orpella, C. Voz, D. Peiró, J. Bertomeu, L.F. Marsal, J. Pallarés, J. Andreu, R. Alcubilla, Mater. Sci. Eng. B 69/70 (2000) 526.
- [14] R.A. Street, Hydrogenated amorphous silicon, Cambridge University Press, Cambridge, 1991, p. 136.

Table 1. Filament temperature (T_F), substrate temperature (T_S), pressure (p), silane flow (ϕ_{SiH_4}), phosphorus or boron to silicon atomic ratio in gas phase ($[\text{P}]/[\text{Si}]$ and $[\text{B}]/[\text{Si}]$) and hydrogen dilution ($\phi_{\text{H}_2}/\phi_{\text{Tot}}$) for the samples shown in this study. The first character in the label of the samples stands for amorphous (A) or nanocrystalline (C), and the second for the type of doping (N-type or P-type).

Sample	T_F (°C)	T_S (°C)	p (mbar)	ϕ_{SiH_4} (sccm)	$[\text{P}]/[\text{Si}]$ (%)	$[\text{B}]/[\text{Si}]$ (%)	$\phi_{\text{H}_2}/\phi_{\text{Tot}}$ (%)
AN	1640	200	3.0×10^{-2}	4	1.0	-	0
AP1	1640	125	3.8×10^{-2}	4	-	1.0	33
AP2	1900	450	1.2×10^{-2}	10	-	1.0	33
CN	1740	225	7.0×10^{-3}	2	1.6	-	89
CP1	1740	175	7.0×10^{-3}	2	-	1.6	89
CP2	1740	125	1.0×10^{-2}	4	-	0.8	93

Table 2. Crystalline fraction as deduced from Raman measurements, dark conductivity at 30°C and activation energy of the dark conductivity of the films.

Sample	X_C	$\sigma_{30^\circ\text{C}}$ (S cm ⁻¹)	E_A (eV)
AN	0	1.6×10^{-2}	0,23
AP1	0	3.3×10^{-6}	0,64
AP2	0	9.1×10^{-6}	0,47
CN	0,91	9,8	0,02
CP1	0,59	0,74	0,06
CP2	0,93	1,7	0,03

Figure Captions

Figure 1. Raman spectra of the samples presented in this study.

Figure 2. Arrhenius plots corresponding to the p-doped amorphous (right axis) and nanocrystalline (left axis) films. The activation energy of the dark conductivity has been determined from the cooling part of the plots.

Figure 3. Dark conductivity at 30°C of several p-doped samples from doping gas phase ratios around 1% as a function of the crystalline fraction of the films.

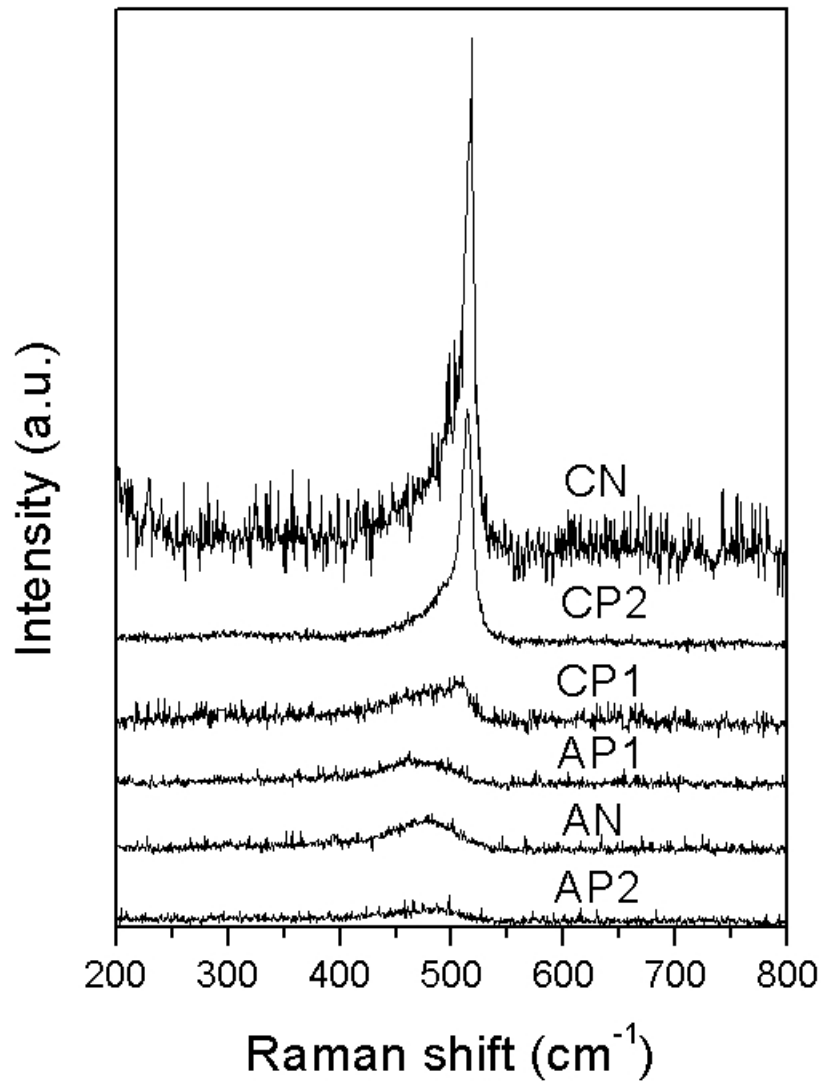


Figure 1. "Investigations on ...", M. Fonrodona et al.

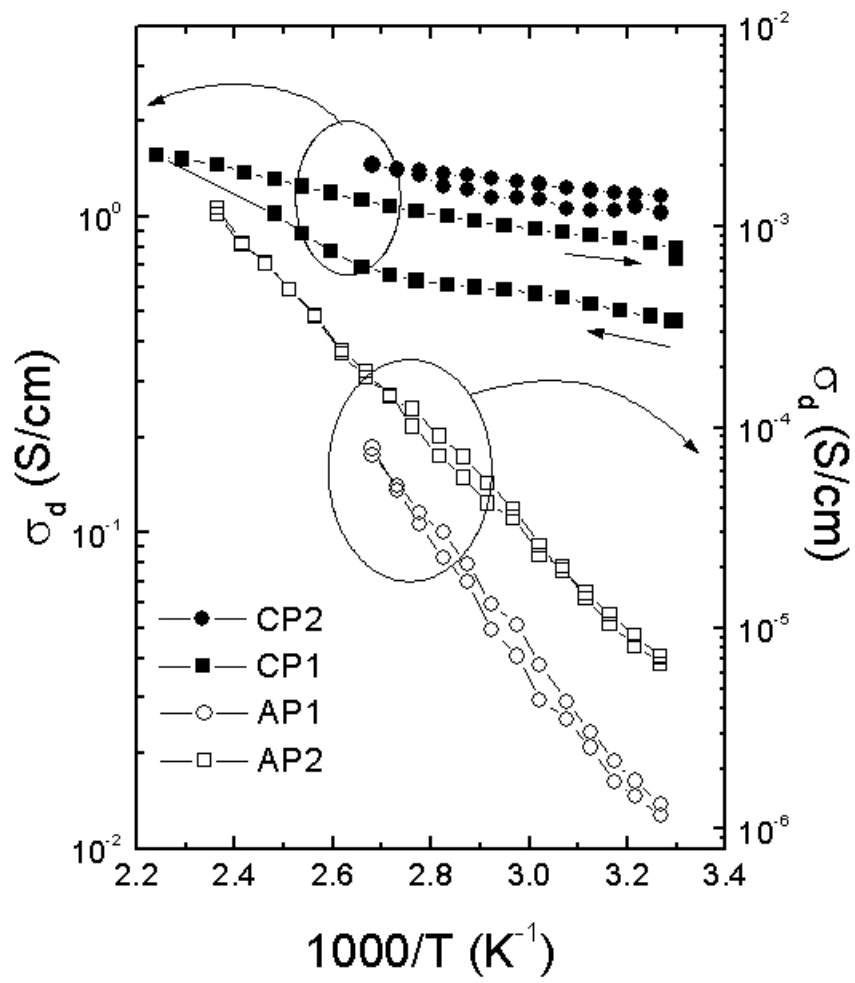


Figure 2. "Investigations on ...", M. Fonrodona et al.

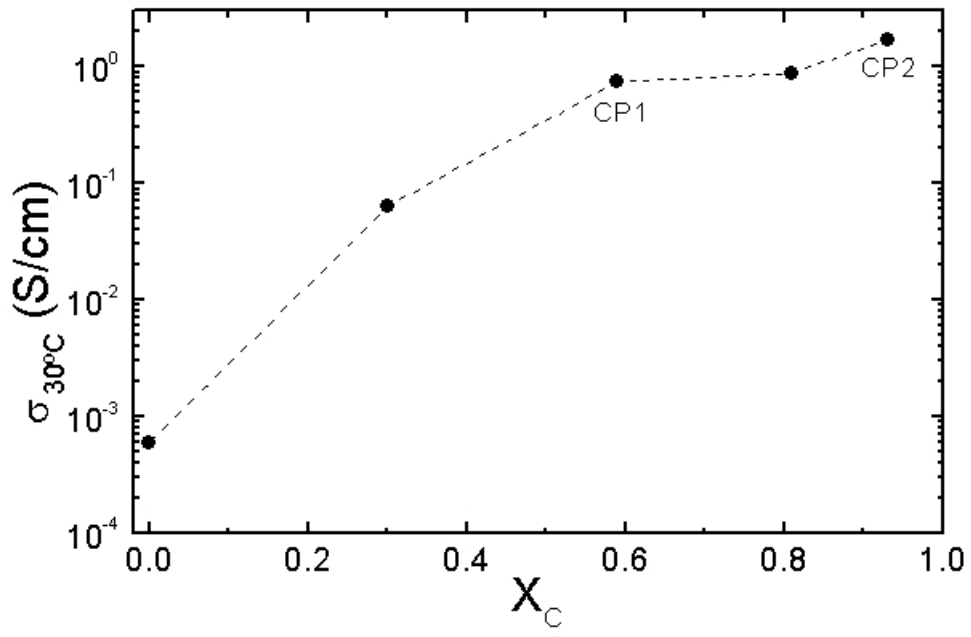


Figure 3. "Investigations on ...", M. Fonrodona et al.